

Structural Study on *O*-Glycopeptides: Glycosylation-Induced Conformational Changes of *O*-GlcNAc, *O*-LacNAc, *O*-Sialyl-LacNAc, and *O*-Sialyl-Lewis-X Peptides of the Mucin Domain of MAdCAM-1

Wen-guey Wu,[†] Laura Pasternack, Dee-Hua Huang, Kathryn M. Koeller, Chun-Cheng Lin, Oliver Seitz, and Chi-Huey Wong*

Contribution from the Department of Chemistry and the Skaggs Institute for Chemical Biology, The Scripps Research Institute, 10550 North Torrey Pines Road, La Jolla, California 92037

Received September 29, 1998

Abstract: A combined NMR and computer modeling approach is applied to study and compare the structures of *O*-sialyl-Lewis-X (SLe^x) and its synthetic intermediates attached to an octapeptide fragment of the mucin domain of MAdCAM-1. The conformation of the carbohydrate moiety of the *O*-SLe^x peptide is found to be the same as that of free SLe^x. The conformation of the polypeptide backbone and the orientation of the carbohydrate moiety relative to the peptide bond, however, depend on the extent of glycosylation. Glycosylation-induced conformational change of the octapeptide from a random structure to a turn-like structure was observed. The extent of glycosylation appears to have a subtle effect on the turn structure, including the dynamics of *cis*–*trans*-proline isomerization. On the basis of structural constraints obtained from the NMR study, computer modeling and molecular dynamics calculations were then used to obtain low-energy conformations of the glycopeptides. The conformational differences observed between the individual glycopeptides can be rationalized as a balance between hydrophobic (carbohydrate–peptide) and hydrophilic (carbohydrate–carbohydrate and carbohydrate–water) interactions. These differences provide some insight into the conformational specificity of glycosyltransferases used in this study. Comparison of the structure of the polypeptide backbone in the presence and absence of carbohydrate attachment also provides an explanation for the lack of N-glycosylation in the Asn-containing mucin domain of MAdCAM-1, as well as for the glycosylation-induced cleavage of the glycopeptide esters linked to a solid support during synthesis.

Introduction

Mucosal addressin cell adhesion molecule-1 (MAdCAM-1) is a complex multidomain glycoprotein comprising several structural motifs, including a serine/threonine-rich region. This “mucin” domain may serve as a backbone to present O-linked carbohydrate ligands to receptors on lymphocytes.¹ Specifically, MAdCAM-1 has been reported to interact with L-selectin in the process of leukocyte trafficking.² Selectin ligands terminating with sialyl-Lewis-X (SLe^x) may be attached to the polypeptide backbone of MAdCAM-1, thereby allowing the glycoprotein to participate in selectin-mediated cell adhesion.

We have recently synthesized β -*O*-SLe^x attached to Thr5 of the octapeptide sequence 227–234 of the mucin domain of MAdCAM-1 (Figure 1A). Oligosaccharides linked to serine or threonine in natural mucin sequences are generally glycosylated through an α linkage to *N*-acetyl galactosamine. Therefore,

although the results of this study cannot be translated directly into the process of MAdCAM-1 mediated cell–cell adhesion, the synthetic effort that provided the glycopeptides studied herein was originally undertaken to accomplish the first synthesis of an O-glycosidically linked SLe^x glycopeptide. During the synthesis, we noted that glycosylation facilitated the release of the glycopeptide from its ester linkage to the solid support (Figure 1B), suggesting that a glycosylation-induced conformational change of the peptide might occur and affect its stability and chemoenzymatic reactivity.⁴ The synthetic *O*-glycopeptide appears to be an interesting model system for the study of the molecular basis of glycosylation-induced conformational change,^{5,6} a topic of current interest in understanding the role of glycosylation in protein structure and function.⁷

There is also much interest in the determination of the structure of SLe^x,^{8–10} one of the minimum carbohydrate structures recognized by E-, P-, and L-selectin.² The establishment of the solution structure⁸ of SLe^x and its selectin-bound^{9,10} form has allowed the rational design of potent SLe^x mimics

* To whom correspondence may be addressed.

[†] On sabbatical leave from Department of Life Sciences, National Tsing Hua University, Taiwan.

(1) Briskin, M. J.; McEvoy, L. M.; Butcher, E. C. *Nature* **1993**, *363*, 461–464.

(2) (a) Malhotra, R.; Bird, M. I. *Chem. Biol.* **1997**, *4*, 543–547. (b) Handa, K.; Stroud, M. R.; Hakomori, S.-I. *Biochemistry* **1997**, *36*, 12412–12420. (c) Wilkins, P. P.; McEver, R. P.; Cummings, R. D. *J. Biol. Chem.* **1996**, *270*, 18732–18742. (d) Kansas, G. S. *Blood* **1996**, *88*, 3259–3287. (e) McEver, R. P.; Moore, K. L.; Cummings, R. D. *J. Biol. Chem.* **1995**, *269*, 11025–11029. (f) Lasky, L. A. *Annu. Rev. Biochem.* **1995**, *64*, 113–139. (g) Varki, A. *Proc. Natl. Acad. Sci. U.S.A.* **1994**, *91*, 7390–7397. (h) Springer, T. A. *Cell* **1994**, *76*, 301–314.

(3) Simanek, E. E.; McGarvey, G. J.; Jablonowski, J. A.; Wong, C.-H. *Chem. Rev.* **1998**, *98*, 833–862.

(4) Seitz, O.; Wong, C.-H. *J. Am. Chem. Soc.* **1997**, *38*, 8766–8776.

(5) (a) O'Connor, S. E.; Imperiali, B. *Chem. Biol.* **1998**, *5*, 427–437.

(b) O'Connor, S. E.; Imperiali, B. *J. Am. Chem. Soc.* **1997**, *119*, 2295–2296.

(6) (a) Liang, R.; Andreotti, H.; Kahne, D. *J. Am. Chem. Soc.* **1995**, *117*, 10395–10396. (b) Andreotti, A. H.; Kahne, D. *J. Am. Chem. Soc.* **1993**, *115*, 3352–3353.

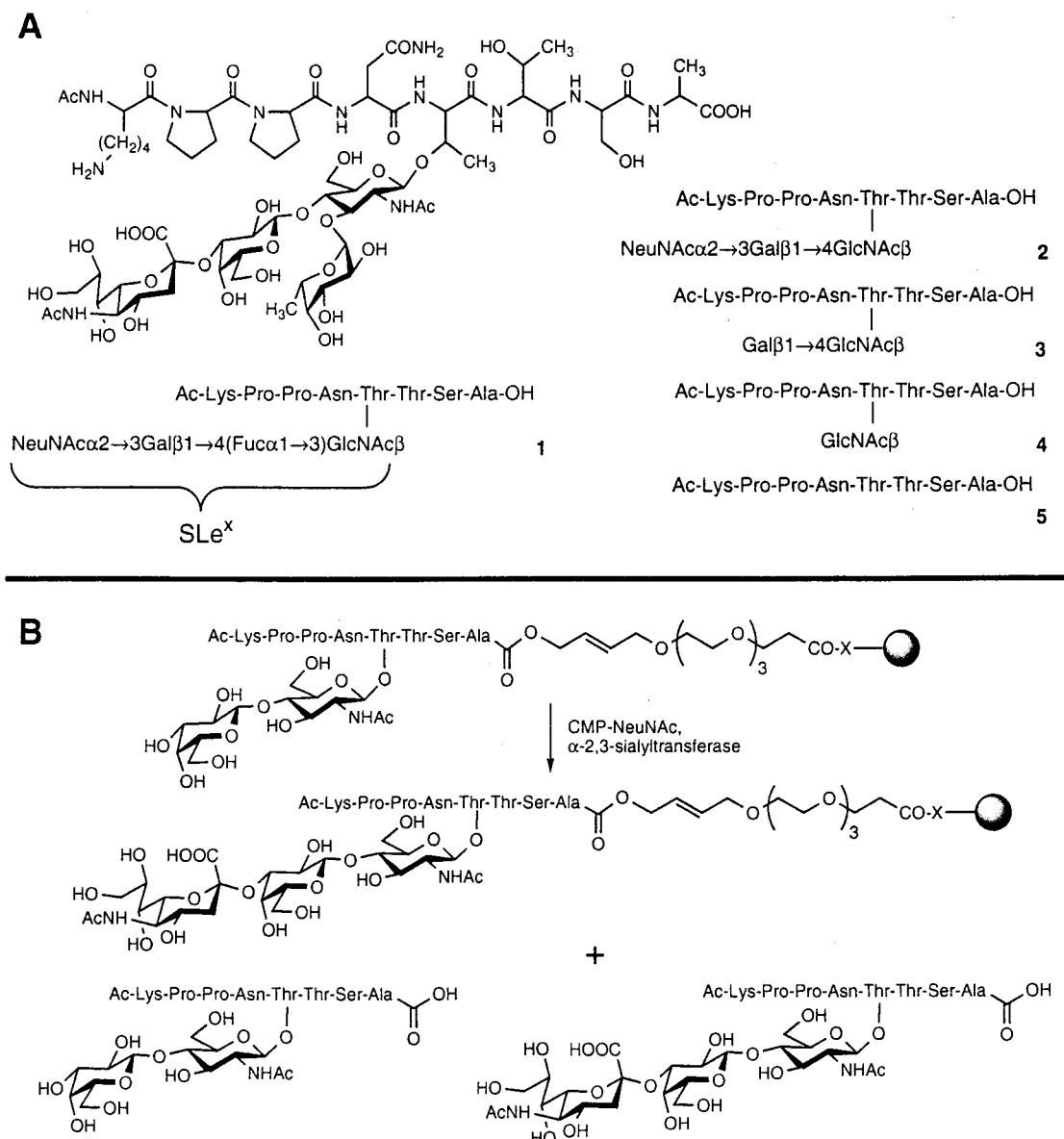


Figure 1. (A) Schematic diagram of the octapeptide of the mucin domain of MADCAM-1 and its related *O*-glycopeptides and (B) representative diagram of the glycosylation-induced ester hydrolysis of the glycopeptide attached to a solid support during enzymatic synthesis. The amino acid sequence 227–234 of the mucin polypeptide domain was attached to various carbohydrate moieties, including SLe^x, via β -*O*-GlcNAc linkage at the indicated Thr position.

suitable for interference of the inflammatory response.^{3,11} The binding affinity of both SLe^x and most of its mimics to selectins are, however, several orders of magnitude weaker than that of the natural ligands, i.e., SLe^x-containing glycoproteins such as MADCAM-1 and PSGL-1 (P-selectin glycoprotein ligand-1).

(7) (a) Pickford, A. R.; Potts, J. R.; Campbell, I. D. *J. Mol. Biol.* **1998**, *276*, 177–187. (b) Rudd, P. M.; Dwek, R. A. *Crit. Rev. Biochem. Mol. Biol.* **1997**, *32*, 1–100. (c) Huang, X.; Barchi, J. J., Jr.; Lung, F.-D. T.; Roller, P. P.; Nara, P. L.; Muschik, J.; Garrity, R. R. *Biochemistry* **1997**, *36*, 10846–10856. (d) Huang, X.; Smith, C.; Berzofsky, J. A.; Barchi, J. J., Jr. *FEBS Letts.* **1996**, *393*, 280–286. (e) Mer, G.; Hietter, H.; Lefevre, J.-F. *Nat. Struct. Biol.* **1996**, *3*, 45–53. (f) Wyss, D. F.; Choi, J. S.; Li, J.; Knoppers, M. H.; Willis, K. J.; Arulanandam, A. R. N.; Smolyar, A.; Reinherz, E. L.; Wagner, G. *Science* **1995**, *269*, 1273–1278. (g) Fletcher, C. M.; Harrison, R. A.; Lachmann, P. J.; Neuhaus, D. *Structure* **1994**, *2*, 185–199. (h) Lis, H.; Sharon, N. *Eur. J. Biochem.* **1993**, *218*, 1–27. (i) Gerken, T. A.; Butenhof, K. J. *Biochemistry* **1993**, *32*, 2650–266. (j) Sticht, H.; Joao, H. C.; Scragg, I. G.; Dwek, R. A. *FEBS Lett.* **1992**, *307*, 343–346. (k) Wormald, M. R.; Wooten, E. W.; Bazzo, R.; Edge, C. J.; Feinstein, A.; Rademacher, T. W.; Dwek, R. A. *Eur. J. Biochem.* **1991**, *198*, 131–139. (l) Shogren, R.; Gerken, T. A.; Jentoft, N. *Biochemistry* **1989**, *28*, 5525–5536. (m) Gerken, T. A.; Butenhof, K. J.; Shogren, R. *Biochemistry* **1989**, *28*, 5536–5543.

As in many cases of carbohydrate–protein interactions,¹² this observation has led to the suggestion that selectin/glycoprotein–ligand affinity may be multivalently enhanced through the presentation of multiple copies of SLe^x along the peptide backbone.

(8) (a) Lin, Y.-C.; Hummel, C. W.; Huang, D.-H.; Ichikawa, Y.; Nicolaou, K. C.; Wong, C.-H. *J. Am. Chem. Soc.* **1992**, *114*, 5452–5454. (b) Ichikawa, Y.; Lin, Y.-C.; Dumas, D. P.; Shen, G.-J.; Garcia-Junceda, E.; Williams, M. A.; Bayer, R.; Ketcham, C.; Walker, L. E.; Paulson, J. C.; Wong, C.-H. *J. Am. Chem. Soc.* **1992**, *114*, 9283–9298. (9) Poppe, L.; Brown, G. S.; Philo, J. S.; Nikrad, P. V.; Shah, B. H. *J. Am. Chem. Soc.* **1997**, *119*, 1727–1736. (10) (a) Scheffler, K.; Brisson, J.-R.; Weisemann, R.; Magnani, J. L.; Wong, W. T.; Ernst, B.; Peters, T. *J. Biomol. NMR* **1997**, *11*, 423–436. (b) Ng, K. K.-S.; Weis, W. I. *Biochemistry* **1997**, *36*, 979–988. (c) Jahnke, W.; Kolb, H. C.; Blommers, M. J. J.; Magnani, J. L.; Ernst, B. *Angew. Chem., Int. Ed. Engl.* **1997**, *36*, 2603–2606. (d) Cooke, R. M.; Hale, R. S.; Lister, S. G.; Shah, G.; Weir, M. P. *Biochemistry* **1994**, *33*, 10591–10596. (11) (a) Wong, C.-H.; Moris-Varas F.; Hung, S.-C.; Marron, T. G.; Lin, C.-C.; Gong, K. W.; Weitz-Schmidt, G. *J. Am. Chem. Soc.* **1997**, *119*, 8152–8158. (b) Kolb, H. C.; Ernst, B. *Chem. Eur. J.* **1997**, *3*, 1571–1578. (12) (a) Lee, Y. C.; Lee, R. T. *J. Biomed. Sci.* **1996**, *3*, 221–237. (b) Lee, Y. C.; Lee, R. T. *Acc. Chem. Res.* **1995**, *28*, 321–327.

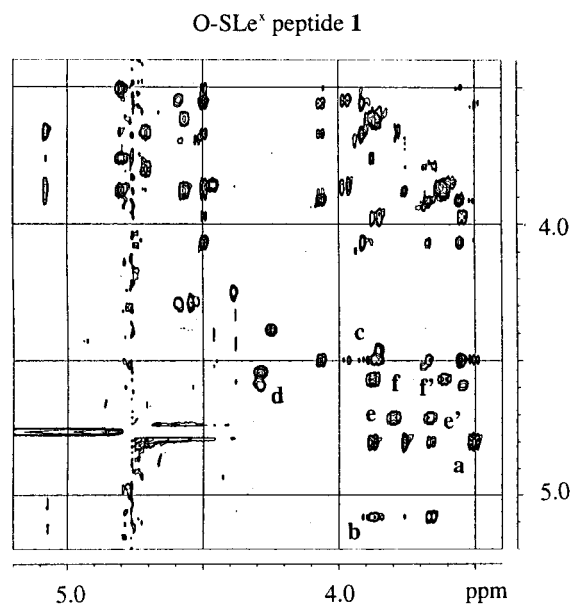


Figure 2. ROESY spectrum of *O*-SLe^x peptide **1** with a mixing time of 300 ms. Representative assignments show characteristic ROESY cross-peaks of SLe^x [a(H5^{Fuc}, H2^{Gal}), b(H1^{Fuc}, H3^{GlcNAc}) and c(H1^{Gal}, H4^{GlcNAc})], trans conformation of the proline residues [e/e' (Pro2 α , Pro3 δ) and f/f' (Lys1 α , Pro2 δ)], and carbohydrate–polypeptide interaction [d(Thr5 H β , H1^{GlcNAc})]. The resonance positions of the representative peaks are (in ppm): a(4.80, 3.50), b(5.08, 3.84), c(4.50, 3.89), d(4.29, 4.60), e/e'(4.71, 3.81/3.66), and f/f'(4.56, 3.88/3.62).

Conformational analysis of galactose-anchored SLe^x dimers has indicated that the conformation within a single SLe^x tetrasaccharide unit in the dimer is the same as that of the SLe^x monomer.¹³ It is, however, not known whether the attachment of polypeptide to SLe^x affects the carbohydrate conformation. We address this question by analyzing the structures of an *O*-SLe^x glycopeptide and its synthetic intermediates (Figure 1) using a combined NMR and computer modeling approach.

Results and Discussion

Conformational Analysis of the Carbohydrate Moiety in *O*-SLe^x Peptide. We have previously determined the conformation of the SLe^x tetrasaccharide and bivalent SLe^x analogues in aqueous solution.^{8,13} It was concluded that SLe^x in both monomeric and bivalent forms adopts the same conformation. In this study, it can also be concluded that the SLe^x tetrasaccharide retains its functional conformation when attached to the octapeptide.

No significant conformational differences were observed between the carbohydrate moiety of *O*-SLe^x peptide **1** in this study and free SLe^x reported previously.^{8,9,13} First and foremost, the ¹H NMR chemical shifts of SLe^x from both samples were found to be similar. Further support for this conclusion comes from examination of the intensity of the cross-peaks in ROESY (rotating frame Overhauser enhancement spectroscopy) spectra (Figure 2). For instance, distance constraints obtained from ROESY experiments for the intercarbohydrate proton pairs (H1^{Fuc}, H3^{GlcNAc}), (H1^{Gal}, H4^{GlcNAc}), and (H3^{Gal}, H3_{ax}^{NeuNAc}) are known to be useful for establishing the periplanar conformation of oligosaccharides when used in conjunction with molecular

dynamics simulation.¹⁴ All three of these ROE cross-peaks are detected in the spectrum of *O*-SLe^x peptide **1**, suggesting a similar conformation when compared with that of the free form of SLe^x in aqueous solution. This evidence is further supported by the presence of characteristic SLe^x ROESY fingerprint cross-peaks of (H5^{Fuc}, H2^{Gal}), (H6^{Fuc}, H2^{Gal}), and (H3^{Fuc}, H6^{Gal}), which indicate a strong dipolar interaction between the fucose and galactose rings as observed in previous NMR studies of SLe^x.

Subsequent NMR experiments were carried out at pH 3.0 to study the exchangeable amide protons. As shown in the NOESY (nuclear Overhauser enhancement spectroscopy) spectrum of *O*-SLe^x peptide **1** in Figure 3, the amide proton of *N*-acetyl glucosamine (GlcNAc) exhibits strong NOEs not only with the intraresidual protons H1, H3, and the acetyl group of GlcNAc but also with the interresidual proton H1 of Fuc. A weak but visible interaction with H2 of Fuc is also observed. The NH proton of GlcNAc also exhibits an NOE with Thr5 H β and H γ . NOE cross-peaks are observed for the amide proton pairs (Asn4, Thr5), (Thr6, Ser7), and (Ser7, Ala8) in the polypeptide backbone of *O*-SLe^x peptide **1**. Out of the six peptide backbone NH protons, only the NH proton of Thr6 exhibits an NOE cross-peak with H2^{GlcNAc} of the carbohydrate moiety. Distance constraints obtained from the exchangeable NH protons were included in molecular dynamics simulations.

A total of 51 interresidual ROE/NOE constraints and ³J_{NH α coupling constants were obtained for *O*-SLe^x peptide **1**. These constraints were subjected to a restrained molecular dynamics simulation utilizing the AMBER force field (modified for glycopeptides).¹⁵ As Homans points out, the use of a full molecular mechanical force field is vital to the molecular modeling of glycopeptides. This is required typically, since NOE data of oligosaccharides is insufficient when used alone and distance geometry calculations result in poor convergence. As shown in Figure 4, the carbohydrate moiety of *O*-SLe^x peptide **1** is indeed similar to that of free SLe^x, despite the attachment of the octapeptide. For instance, the bond angles determined for the linkages Fuc α 1 \rightarrow 3GlcNAc and Gal β 1 \rightarrow 4GlcNAc are 80°/12° and 56°/6°, respectively. These values compare favorably with those previously determined by GESA calculation method for free SLe^x.⁸ The value of the Fuc α 1 \rightarrow 3GlcNAc bond angle deviates slightly from that determined previously. Molecular modeling of free SLe^x using the modified AMBER force field and restrained molecular dynamics, however, indicates that this slight difference is due to the use of a different force field and is not the result of peptide attachment.}

The linkages between NeuNAc and Gal are more variable due to the increased flexibility of this region. We previously applied MM2 and GESA calculations to obtain four possible conformations for the α 2 \rightarrow 3 linkage of the NeuNAc α 2 \rightarrow 3Gal bond of SLe^x which yielded ϕ/ψ angles of A(163°/−57°), B(−170°/−8°), C(−79°/7°), and D(68°/20°). By using the modified AMBER force field and molecular dynamics, we were able to generate similar results with an additional energy-minimized conformation of E(−100°/−50°). The distance constraint imposed by the observed ROESY cross-peak of (H3^{Gal}, H3_{ax}^{NeuNAc}) would exclude substantial contributions of conformers C and D. However, as we will show in the following section, a weak

(14) (a) Martin-Pastor, M.; Espinosa, J. F.; Asensio, J. L.; Jimenez-Barbero, J. *Carbohydr. Res.* **1997**, 298, 15–49. (b) Peters, T.; Pinto, B. M. *Curr. Opin. Struct. Biol.* **1996**, 6, 710–720. (c) Woods, R. J. *Rev. Comput. Chem.* **1996**, 9, 129–165. (d) Boswell, D. R.; Coxon, E. E.; Coxon, J. M. *Adv. Mol. Model.* **1993**, 3, 145–193.

(15) (a) Rutherford, T. J.; Homans, S. W. *Biochemistry*, **1994**, 33, 9609–9614. (b) Rutherford, T. J.; Partridge, J.; Weller, C. T.; Homans, S. W. *Biochemistry* **1993**, 32, 12715–12724. (c) Homans, S. W. *Biochemistry* **1990**, 29, 9110–9118.

(13) (a) DeFrees, S. A.; Kosch, W.; Way, W.; Paulson, J. C.; Sabesan, S.; Halcomb, R. L.; Huang, D.-H.; Ichikawa, Y.; Wong C.-H. *J. Am. Chem. Soc.* **1995**, 117, 66–79. (b) DeFrees, S. A.; Gaeta, F. C. A.; Lin Y.-C.; Ichikawa, Y.; Wong, C.-H. *J. Am. Chem. Soc.* **1993**, 115, 7549–7550.

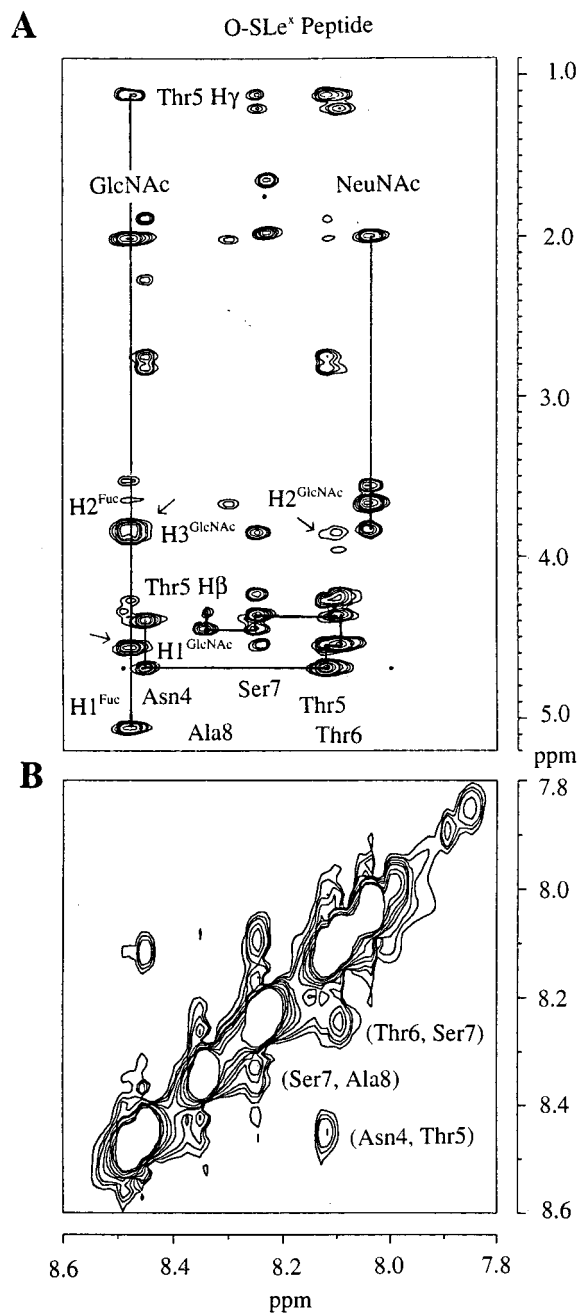


Figure 3. Amide exchangeable proton region of the NOESY spectrum of *O*-SLe^x peptide **1** with mixing time of 300 ms. The sequential assignments of the polypeptide and the NH resonances of the two *N*-acetyl groups in the GlcNAc and NeuNAc carbohydrate moieties are indicated by solid line connection. The arrows indicate the representative assignments of proton resonances from the GlcNAc moiety (panel A). Three glycosylation-induced NOESY cross-peaks in the amide proton region are also shown (panel B).

ROESY cross-peak of (H3^{Gal}, H8^{NeuNAc}) in *O*-SLe^x peptide **1** indicates that more than one stable conformation of SLe^x might be present. Recently, a similar conclusion has been reached based on an NMR study of SLe^x at -15°C .⁹

Glycosylation-Induced Conformational Change of the Carbohydrate Moieties. In a previous study entailing the enzymatic solid-phase synthesis of *O*-SLe^x peptide **1**, unexpected formation of resin-cleaved products was observed (Figure 1B). Although the extent of ester hydrolysis was dependent on the exact oligosaccharide attached to the octapeptide, the unglycosylated octapeptide was stable to hydrolysis. Although all glycosylated peptides demonstrate additional conformational

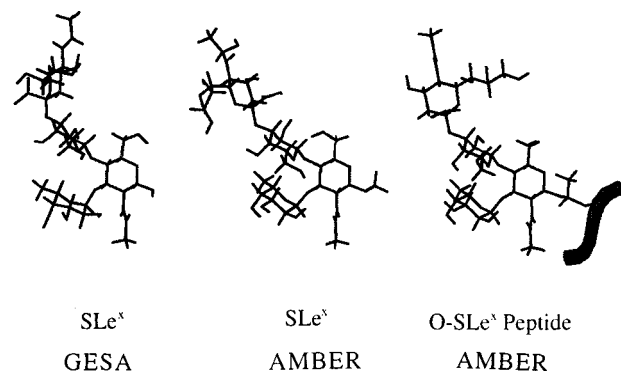


Figure 4. Comparison of the SLe^x structure in the presence and absence of polypeptide attachment. Application of different force fields GESA and AMBER is shown to generate similar structures. Different ϕ/Ψ angles of the NeuNAc α 2 \rightarrow 3Gal bond [from left to right: ($-171^{\circ}/-6^{\circ}$), ($60^{\circ}/0^{\circ}$) and ($-66^{\circ}/-7^{\circ}$)] are chosen for the three presented structures to emphasize the flexibility of the molecule near the region.

stability of the peptide that could explain the hydrolysis reaction, conformational differences are apparent among the individual glycopeptides. This observation indicates that hydrolytic cleavage of the solid support allylic ester bond might be caused by a carbohydrate-induced specific conformational change of the peptide.

As shown in Figure 5, we use the two methyl groups of Thr5 and Thr6 and their observed dipolar interaction with the neighboring GlcNAc to illustrate the conformational differences among the glycopeptides. In *O*-GlcNAc peptide **4**, significant ROESY cross-peaks can be observed not only between the methyl group of Thr6 and H2^{GlcNAc} and H4^{GlcNAc} but also between the methyl group of Thr5 and H1^{GlcNAc}. After further glycosylation, i.e., attaching Gal to GlcNAc in a β 1 \rightarrow 4 linkage, the methyl group of Thr6 in *O*-LacNAc peptide **3** now exhibits a new NOE with H5^{GlcNAc} and loses the NOEs with H2^{GlcNAc} and H4^{GlcNAc}. While sialylation of the LacNAc peptide produces no further change of the ROESY pattern (data not shown), all ROESY cross-peaks between GlcNAc and the methyl group of Thr6 disappear after α 1 \rightarrow 3 fucosylation of GlcNAc to form *O*-SLe^x peptide **1**. In addition, as emphasized by the arrows shown in Figure 5B, the strong ROESY cross-peak (H1^{GlcNAc}, Thr5 H γ), seen in the spectrum of *O*-GlcNAc and *O*-LacNAc peptides **4** and **3**, becomes significantly reduced in the case of *O*-SLe^x peptide **1**. These observations provide strong evidence supporting the sequence-specific reorientation of the carbohydrate moiety relative to the peptide in these β -*O*-GlcNAc linked glycopeptides. The structures obtained by molecular dynamics simulation as depicted in Figure 5A demonstrate how reorientation of the GlcNAc group might account for the observed change of the ROE pattern. With each subsequent glycosylation necessary to building the SLe^x core, the GlcNAc moiety reorients and becomes more exposed to the aqueous medium.

Hydrophobic interactions between amino acid side chains and the carbohydrate ring have recently been established as an important factor in anchoring carbohydrate moieties against polypeptide chains.¹⁶ In this study, anchoring GlcNAc via the two hydrophobic methyl groups of two consecutive Thr residues

(16) (a) Lis, H.; Sharon, N. *Chem. Rev.* **1998**, *98*, 637–674. (b) Drickmer, K. *Structure* **1997**, *5*, 465–468. (c) Elgavish, S.; Shaanan, B. *Trends Biochem. Sci.* **1997**, *22*, 462–467. (d) Weis, W. I.; Drickmer, K. *Annu. Rev. Biochem.* **1996**, *65*, 441–473. (e) Kolatkar, A. R.; Weis, W. I. *J. Biol. Chem.* **1996**, *271*, 6679–6685. (f) Rini, J. M. *Annu. Rev. Biophys. Biomol. Struct.* **1995**, *24*, 551–577. (g) Nelson, R. M.; Venot, A.; Bevilacqua, M. P.; Linhardt, R. J.; Stamenkovic, I. *Annu. Rev. Cell Dev. Biol.* **1995**, *11*, 601–631. (h) Bourne, Y.; van Tilbeurgh, H.; Cambillau, C. *Curr. Opin. Struct. Biol.* **1993**, *3*, 681–686.

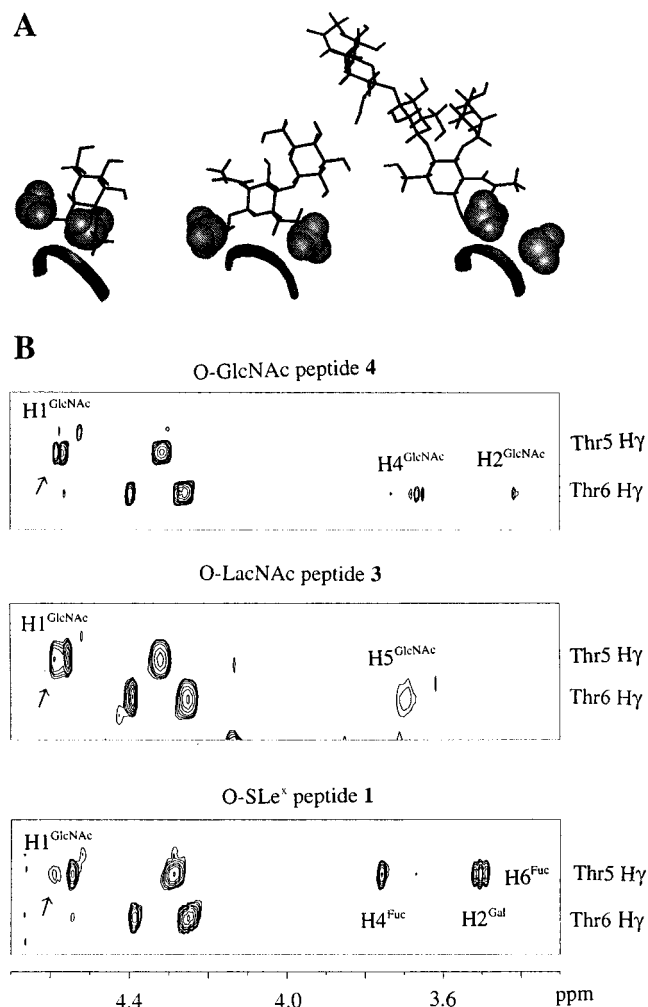


Figure 5. (A) Molecular models of *O*-GlcNAc peptide 4, *O*-LacNAc peptide 3, and *O*-SLe^x peptide 1 and (B) ROESY cross-peaks of the GlcNAc protons with the two methyl groups of Thr5 and Thr6. The two strong cross-peaks in the right-hand side of the ROESY spectrum of *O*-SLe^x peptide 1 are assigned to (H4^{Fuc}, H6^{Fuc}) and (H2^{Gal}, H6^{Fuc}). Both cross-peaks can also be identified in polypeptide-free SLe^x. The angles of the C α -C β bond for the glycosylated Thr5 are found to be relatively restricted for *O*-GlcNAc peptide 4 and *O*-SLe^x peptide 1 (-66° and 65° , respectively), whereas several different conformations are possible for *O*-LacNAc peptide 3.

provides additional support for the important role of hydrophobic contacts in carbohydrate-peptide interactions. The addition of carbohydrate residues onto the GlcNAc moiety is expected to increase its hydrophilicity, making carbohydrate-water interactions more favorable than carbohydrate-peptide interactions. Glycosylation-induced reorientation of the GlcNAc moiety can then be understood as a competition between hydrophobic and hydrophilic forces. To accommodate the more hydrophilic *O*-SLe^x tetrasaccharide in the glycopeptide, the GlcNAc residue reorients to allow more extensive exposure to the aqueous environment.

Additional experimental data indicates a more specific carbohydrate-carbohydrate interaction may also be involved in the aforementioned glycosylation-induced reorientation of the GlcNAc moiety. As shown in Figure 6, $^3J_{\text{NH}\alpha}$ values for the NH in the *N*-acetyl group of several carbohydrate analogues were measured. As indicated, the value of $^3J_{\text{NH}\alpha}$ in *O*-LacNAc peptide 4 is 8.6 Hz, reduced from the expected value of 9.6 Hz observed for *O*-SLe^x peptide 1. The effect can be detected in both the polypeptide-attached and the polypeptide-free carbo-

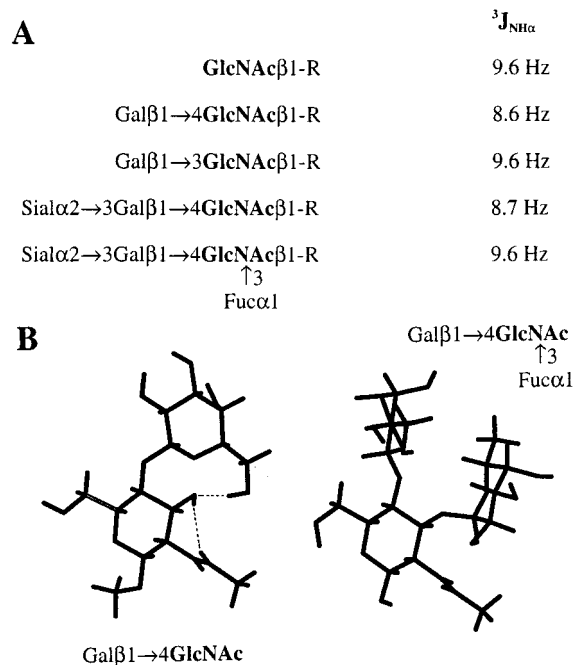


Figure 6. (A) $^3J_{\text{NH}\alpha}$ coupling constants of the *N*-acetyl group of GlcNAc for the studied carbohydrate analogues. (B) Energy-minimized molecular model of two carbohydrate analogues to illustrate the involvement of the 3-OH of GlcNAc as a hydrogen-bonding bridge between the 6-OH of Gal and the carbonyl group of GlcNAc. Fucosylation is seen to eliminate the proposed hydrogen-bonding bridge.

hydrate moiety of GlcNAc, suggesting that the change reflects a galactosylation-induced conformational change of the *N*-acetyl group in GlcNAc. Previous studies employing the Karplus equation¹⁷ have demonstrated the relationship between $^3J_{\text{NH}\alpha}$ values and dihedral angles in protein. Accordingly, our observed decrease in $^3J_{\text{NH}\alpha}$ in a carbohydrate system is consistent with the NH group tilting from an all trans conformation by approximately 30 degrees.

Examination of the ROESY cross-peaks against the NH proton of GlcNAc indicates that the reduction of $^3J_{\text{NH}\alpha}$ value corresponds well with a shift of the ROESY cross-peak pattern from (H1^{GlcNAc}, H3^{GlcNAc}) to (H1^{GlcNAc}, H2^{GlcNAc}). This suggests that the NH group moves toward H1 instead of H3 of GlcNAc during the process of conformational change. Apparently, a free hydroxyl group at the C3 position of GlcNAc is involved in the observed change, since either fucosylation or galactosylation with α 1 \rightarrow 3 or β 1 \rightarrow 3 linkage, respectively, results in a $^3J_{\text{NH}\alpha}$ value of 9.6 Hz (Figure 6A). The energy-minimized structures of the Gal β 1 \rightarrow 4GlcNAc β 1 linkage as shown in Figure 6B suggest that the 3-OH group of GlcNAc may function as a hydrogen-bonding bridge between the 6-OH of Gal and the *N*-acetyl carbonyl group of GlcNAc. This would account for the observed glycosylation-induced conformational change of the *N*-acetyl group. In accordance with the $^3J_{\text{NH}\alpha}$ measurements, the detected conformational change is not possible if the 3-OH group of GlcNAc is glycosylated.

The *N*-acetyl groups of carbohydrates were shown to be rigid for *N*-glycosylated polypeptides of hen ovomucoid.¹⁸ They have also been suggested as playing an important role in promoting the more compact β -turn conformation in *N*-glycopeptides of influenza hemagglutinin A through steric interactions.⁵ In this

(17) Pardi, A.; Billeter, M.; Wuthrich, K. *J. Mol. Biol.* **1984**, *180*, 741-751.

(18) Davis, J. T.; Hirani, S.; Bartlett, C.; Reid, B. R. *J. Biol. Chem.* **1994**, *269*, 3331-3338.

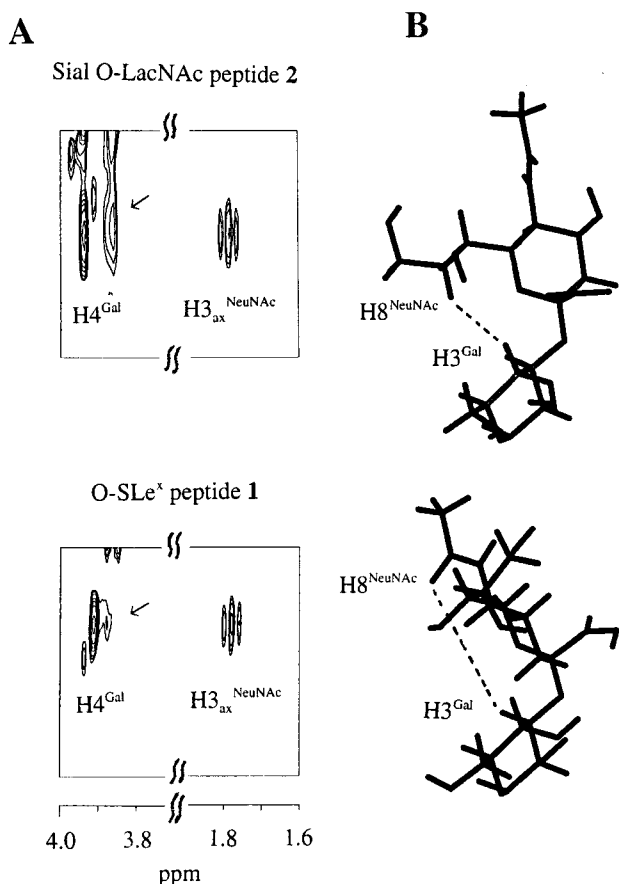


Figure 7. (A) Effect of fucosylation on the ROESY cross-peak between H3 of galactose and H8 of sialic acid and (B) two representative conformations of the NeuNAc α 2 \rightarrow 3Gal bond with ϕ/Ψ angles of ($-98^\circ/-53^\circ$) and ($-159^\circ/-20^\circ$). The arrows shown in panel A indicate the resonance position of the ROESY cross-peak of (H3^{Gal}, H8^{NeuNAc}). The distance between H3 of galactose and H8 of sialic acid is seen to change from 3.25 to 5.7 Å to account for the change of the NOE intensity.

study of a β -O-linked glycopeptide of the mucin domain, we find that the acetyl group in β -O-GlcNAc is also rigid, but its orientation may be modulated by additional glycosylation in a specific manner. In fact, the *N*-acetyl group of carbohydrates is unique not only in its role as a hydrogen bond donor and acceptor¹⁹ but also in providing a hydrophobic methyl group in the region. The *N*-acetyl group of the carbohydrate may therefore play a delicate role in balancing hydrophobic interactions and hydrogen bond formation in protein-carbohydrate and carbohydrate-carbohydrate interactions.

Finally, fucosylation on sialyl *O*-LacNAc is found to change the conformation of the sialyl group relative to LacNAc, as evidenced by the significant intensity change of the ROESY cross-peak of (H3^{Gal}, H8^{NeuNAc}) (Figure 7A). In recent studies of the E-selectin-bound SLe^x conformation^{9,10} it has been noted that the ROESY cross-peaks detected at (H3^{Gal}, H8^{NeuNAc}) and (H3^{Gal}, H3_{ax}^{NeuNAc}) actually represent different orientations of the NeuNAc α 2 \rightarrow 3Gal bond. In previous studies, the ROESY cross-peak of (H3^{Gal}, H8^{NeuNAc}) was detectable in spectra of

the selectin-bound form of SLe^x, whereas that of (H3^{Gal}, H3_{ax}^{NeuNAc}) was found in spectra of free SLe^x. Different conformations of the selectin-bound form of SLe^x can further be distinguished based on the presence and/or absence of other NOE constraints.⁹ Indeed, SLe^x may bind to L-selectin with conformation E($-100^\circ/-50^\circ$) and exhibit NOE cross-peaks of both (H3^{Gal}, H8^{NeuNAc}) and (H3^{Gal}, H3_{ax}^{NeuNAc}). Considering the flexibility of the NeuNAc α 2 \rightarrow 3Gal bond, it is possible that several conformations are present. On the basis of the data obtained in this study, it is not feasible to distinguish whether a dominant carbohydrate conformation of sialyl *O*-LacNAc peptide 2 constitutes the significant enhancement of its NOESY intensity of (H3^{Gal}, H8^{NeuNAc}) as emphasized by the arrows shown in Figure 7A. Nevertheless, the observed spectroscopic change suggests strongly that fucosylation of sialyl *O*-LacNAc peptide 2 to generate *O*-SLe^x peptide 1 alters the conformation of the NeuNAc α 2 \rightarrow 3Gal bond significantly, probably in favor of the SLe^x conformation free in solution.

Glycosylation-Induced Conformational Change of the Polypeptide Chain. Octapeptide. Within the octapeptide sequence of this mucin domain, a potential N-glycosylation site (Asn4-Xaa5-Thr6) has been identified.²⁰ In fact, there are three potential N-linked glycosylation sites in the full-length mucin domain of MAdCAM-1, but biochemical studies suggest that they may not be N-glycosylated. Instead, it was proposed that O-linked carbohydrates are the biological modification of MAdCAM-1.¹ The exact reason that MAdCAM-1 preferentially accepts O-linked carbohydrates instead of N-glycosylation is not known. Since the presence of an Asx-turn has been suggested to play an important role in Asn-linked glycosylation,²⁰ it is of interest to examine whether the potential N-glycosylation site in the mucin domain of MAdCAM-1 can adopt such a conformation. In addition, characterization of the conformation of the glycopeptide used in this study may also shed some light on the glycosylation-induced hydrolytic cleavage of the octapeptide from the solid support during its chemoenzymatic synthesis.

Theoretical and experimental analysis of model peptides and crystallized proteins have suggested that an Asx-turn, involving the side-chain carbonyl group of Asn in a 10-membered cycle, is intrinsically stable as a β -turn.²¹ Such Asx-turns have been detected by NMR methods.²⁰ However, our NMR data argue against the presence of an Asx turn in the Asn-Xaa-Thr sequence motif of octapeptide 5.

First, the $^3J_{\text{HN}\alpha}$ coupling constant of Asn is expected to be in the range of 8–10 Hz for an Asx-turn,²⁰ but our measured value is 6.6 Hz. In fact, the $^3J_{\text{HN}\alpha}$ coupling constants of Asn4 for all five peptides examined in this study fall in the range of 6.6–6.8 Hz.

Second, in an Asx-turn, the amide proton of Thr6 would be expected to be relatively shielded from the solvent due to hydrogen bonding with the Asn side-chain carbonyl group. As shown in Figure 8A, however, NH protons from Asn4, Thr5, Thr6, and Ser7 of octapeptide 5 appear to exchange significantly on an intermediate time-scale, as judged from the extent of exchange-induced linebroadening of the NMR line width at pH 7.0. By this criteria, the amide NH proton of Thr6 appears to be accessible to solvent and is probably not involved in the formation of an Asx-turn structure.

(19) (a) Fowler, P.; Bernet, B.; Vasella, A. *Helv. Chim. Acta* **1996**, *79*, 269–287. (b) Avalos, M.; Babiano, R.; Duran, C. J.; Jimenez, J. L.; Palacios, J. C. *J. Chem. Soc., Perkin Trans. 2* **1992**, 2105–2215. (c) Levery, S. B.; Holmes, E. H.; Harris, D. D.; Hakomori, S.-I. *Biochemistry* **1992**, *31*, 1069–1080. (d) Cagas, P.; Kaluarachchi, K.; Bush, C. A. *J. Am. Chem. Soc.* **1991**, *113*, 6815–6822. (e) Maeji, N. J.; Inoue, Y.; Chujo, R. *Biopolymers* **1987**, *26*, 1753–1767. (f) Scott, J. E.; Heatley, F.; Moorcroft, D.; Alavesen, A. H. *Biochem. J.* **1981**, *199*, 829–832.

(20) (a) Imperiali, B. *Acc. Chem. Res.* **1997**, *30*, 452–459. (b) Imperiali, B.; Spencer, J. R.; Struthers, M. D. *J. Am. Chem. Soc.* **1994**, *116*, 8424–8425. (c) Imperiali, B.; Shannon, K. L.; Unno, M.; Rickert, K. W. *J. Am. Chem. Soc.* **1992**, *114*, 7944–7945. (d) Imperiali, B.; Shannon, K. L. *Biochemistry* **1991**, *30*, 4374–4380.

(21) Abbadi, A.; Mcharfi, M.; Aubry, A.; Premilat, S.; Boussard, G.; Marraud, M. *J. Am. Chem. Soc.* **1991**, *113*, 2729–2735.

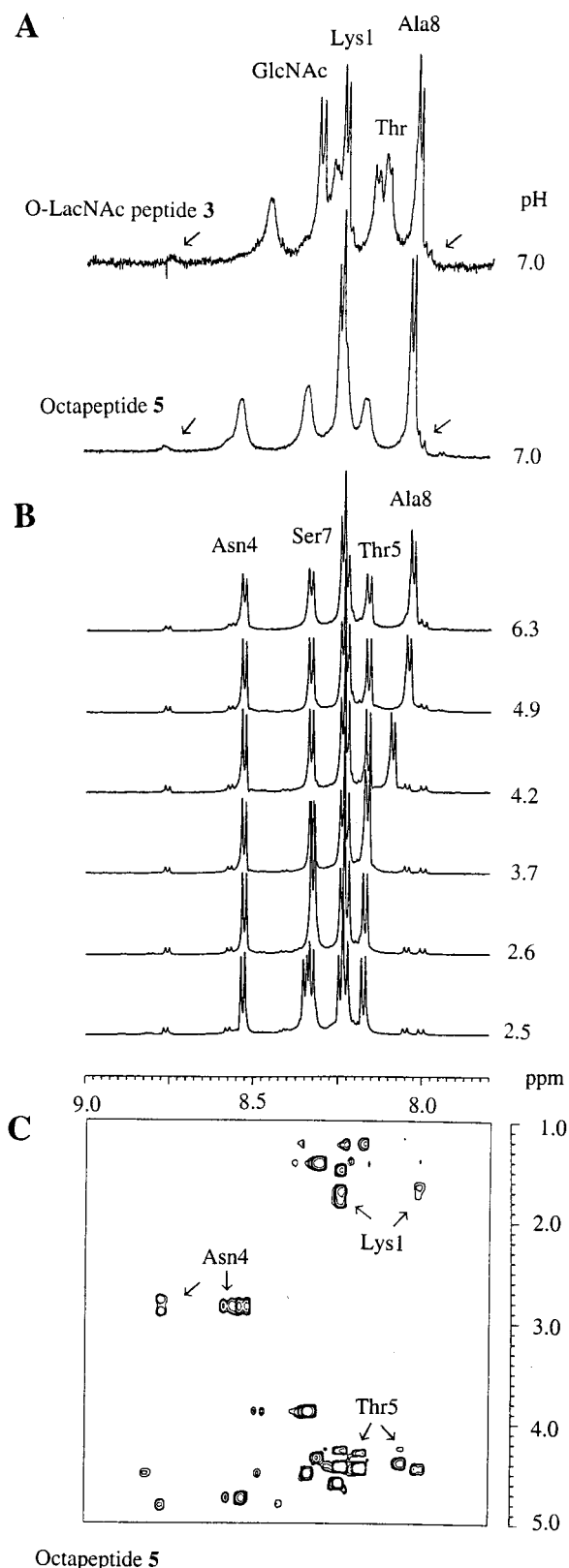


Figure 8. (A) Comparison of the 1D ^1H NMR spectra of *O*-LacNAc peptide 3 and octapeptide 5 in the amide proton region, (B) determination of the pK_a of C-terminal Ala8 by pH titration of octapeptide 5, and (C) TOCSY 2D spectra of octapeptide 5 for the assignment of NMR peaks. Minor components of NMR peaks associated with the proline isomerization conformer can be assigned to Thr5, Asn4, and Lys1.

Finally, a weak ROESY cross-peak of (Thr5, Thr6) has been suggested to be present for an Asx-turn,²⁰ but we did not observe

any ROESY NH–NH cross-peaks in the spectra of octapeptide 5. Although the invisibility of this diagnostic cross-peak could be due to serious overlapping of the chemical shifts of the two Thr NH signals, another Asx-turn predicted cross-peak of (Asn4, Thr5) is also absent. Therefore, our NMR data is consistent with the absence of any significant amount of Asx-turn in the Asn-Xaa-Thr sequence of octapeptide 5. If the positioning of the Asn group within the Asx-turn is essential for the action of oligosaccharyl transferase, the result could explain why the mucin domain of MAdCAM-1 is not N-glycosylated.

Glycopeptides. Glycosylation induces significant changes in chemical shifts for amide protons in the octapeptide backbone except for those of Ala8 and Lys1. For instance, the chemical shifts of the Asn4 NH proton is shifted upfield by 0.08 ppm, and the Ser7 NH proton's resonance is shifted downfield by 0.08 ppm. Although the resonance signals of NH protons of Lys1, Asn4, and Ala8 show similar exchange broadening on both *O*-LacNAc peptide 3 and octapeptide 5, the resonance signals for Thr5 and Thr 6 NH protons in *O*-LacNAc peptide 3 experienced less exchange broadening, compared to those in octapeptide 5 (Figure 8A). This suggests that NH protons for Thr5 and Thr6 are less accessible to solvent and have relatively slower exchange rates compared to the same NH protons in the octapeptide. Both observations suggest that glycosylation induces significant conformational change on the octapeptide backbone. This conformational change will be discussed in more detail in the following sections.

C-Terminal Region. To study the effect of glycosylation on the C-terminal conformation, we performed a pH titration study to see whether the pK_a value of the titratable carboxyl group might be affected. Any significant change in conformation near this region is expected to change the electrostatic environment of the carboxyl group. As shown in a series of ^1H NMR spectra of octapeptide 5 at indicated pH (Figure 8B), only the chemical shift of Ala8 varies as a function of pH, with an apparent pK_a of ~ 3.6 . Similar results, and the same pK_a of ~ 3.6 , were observed in the pH titration study of *O*-LacNAc peptide 3 (data not shown). These studies suggest that glycosylation does not change the conformation of the octapeptide at the C-terminal region.

N-Terminal Region. There are two proline residues near the N-terminal region of the octapeptide. The *cis*–*trans* isomerization of Pro residues is expected to produce structural heterogeneity of the polypeptide backbone.²² Since the amino acid sequences of most O-linked glycoproteins consist of Pro residues near the glycosylation site, it is of interest to examine how glycosylation affects the dynamics of *cis*–*trans* isomerization in the peptide structure.

As shown in Figure 8C, the TOCSY (total correlation spectroscopy) spectrum of octapeptide 5 allows the assignment of some of the minor forms of NH resonances from Lys1, Asn4, and Thr5. On the basis of the signal intensity obtained for the fully relaxed 1D spectrum, it is estimated that 8–10% of the total conformation is a minor form of the polypeptide chain with *cis*-Pro conformation, relative to the major *trans*-Pro form. A similar conclusion can also be made on the basis of signals in the nonexchangeable resonance region (Figure 9). The determined ratio of *cis*/*trans* population falls in the normal range of previously reported values.²²

The attachment of GlcNAc and LacNAc to the octapeptide has no significant effect on the *cis* population. The signal

(22) (a) Dyson, H. J.; Rance, M.; Houghten, R. A.; Lerner, R. A.; Wright, P. E. *J. Mol. Biol.* **1988**, *201*, 161–200. (b) Wuthrich, K.; Billeter, M.; Braun, W. *J. Mol. Biol.* **1984**, *180*, 715–740.

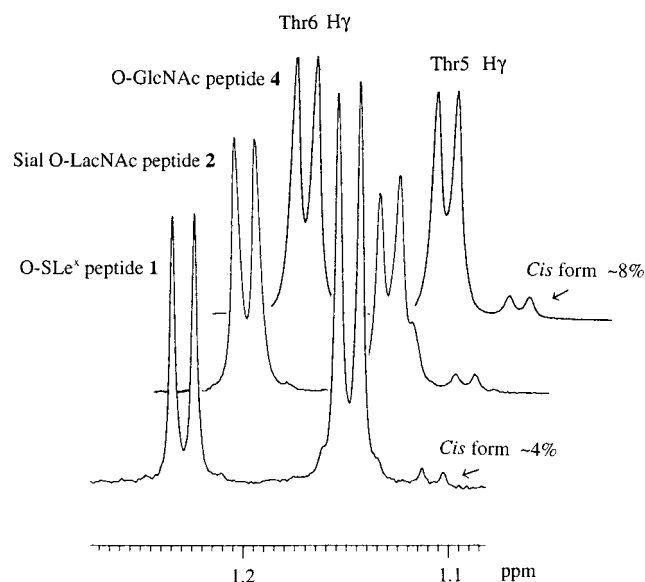


Figure 9. Effect of glycosylation on the population of polypeptide with *cis*-proline conformation as revealed by the signal intensity of the methyl group from the Thr residue.

intensity of the minor form, as pointed out by the arrows shown in Figure 8A, remains similar between the spectra obtained for *O*-LacNAc peptide 3 and octapeptide 5. However, as demonstrated in Figure 9, the final fucosylation step reduces the *cis* population from 8 to 4%. Since the Pro residues are two amino acid positions away from the glycosylation site, this effect may be considered significant. Other similar studies regarding the effect of phosphorylation on the *cis*–*trans* dynamics of polypeptides of Pro-directed protein kinase report results of a similar magnitude.²³ One possible explanation for the reduced population of *cis* conformer in this study is that the last step of glycosylation produces a branched-chain carbohydrate moiety with a bulky group near the glycosylation site. In this respect, steric effects may be mainly responsible for the reduction of the *cis* population.

NMR studies of the conformations of the glycosylated and nonglycosylated loop peptides of the *n*-acetylcholine receptor α -subunit revealed that *N*-glycosylation had a significant effect on the conformational dynamics of the system.²⁴ Specifically, glycosylation significantly altered the *cis*–*trans*-proline equilibrium, favoring the *trans* isomer. In this β -*O*-linked glycosylation study, a reduction of the *cis*/*trans* ratio is only observable after the attachment of a carbohydrate moiety with a branched chain. It is noteworthy that phosphorylation of the polypeptide of Pro-directed protein kinase also alters the *cis*–*trans*-proline equilibrium, although favoring the *cis* isomer, presumably by introducing acidic functionality near the region.²³ In light of the mounting evidence that *O*-glycosylation with GlcNAc is an important regulatory modification that has a reciprocal relationship to *O*-phosphorylation,²⁵ future systematic structural comparison may reveal the interesting reciprocal roles between *O*-glycosylation and *O*-phosphorylation of nuclear and cytoplasmic glycoproteins.

Glycosylation Region. Figure 10 shows the ROESY pattern for four of the studied polypeptides near the NH proton region. At room temperature and pH 3.0, β -*O*-GlcNAc attachment (*O*-

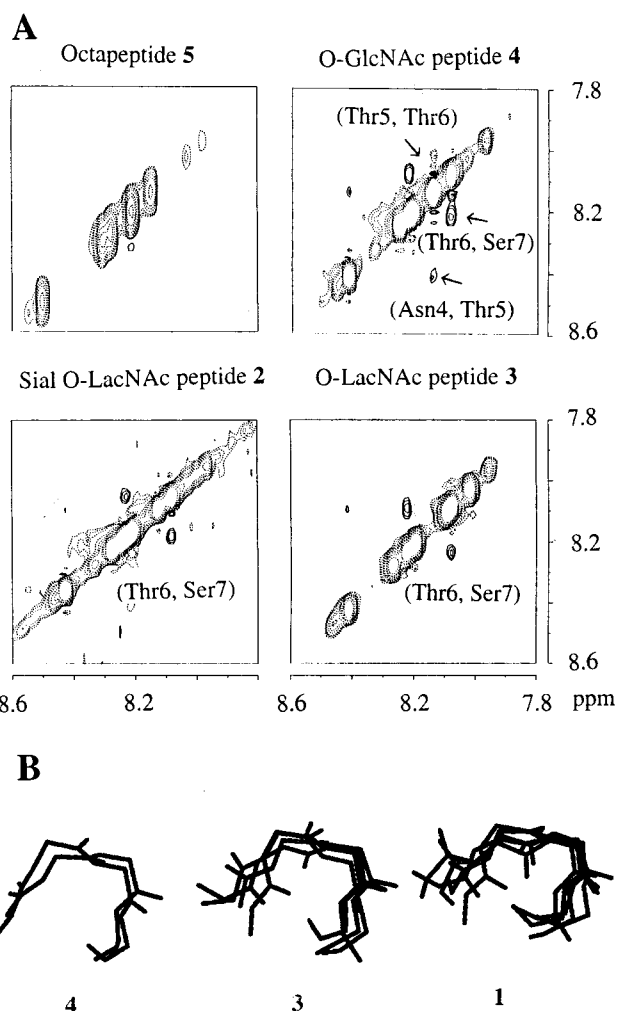


Figure 10. (A) ROESY cross-peaks of octapeptide 5, *O*-GlcNAc peptide 4, *O*-LacNAc peptide 3, and sialyl *O*-LacNAc peptide 2 in the amide proton region and (B) energy-minimized conformations of *O*-GlcNAc peptide 4, *O*-LacNAc peptide 3, and *O*-SLe^x peptide 1 near the glycosylation site. Only the polypeptide backbone of Asn4-Thr5-Thr6-Ser7 is illustrated.

GlcNAc peptide 4) clearly produces three ROESY cross-peaks at (Asn4, Thr5), (Thr5, Thr6), and (Thr6, Ser7) which are all absent in the non-glycosylated octapeptide. With further glycosylation, such as in the cases of sialyl *O*-LacNAc peptide 2 and *O*-LacNAc peptide 3, the ROESY cross-peaks of (Asn4, Thr5) and (Thr5, Thr6) decrease significantly, while that of (Thr6, Ser7) remains essentially the same. *O*-SLe^x peptide 1 exhibits NOESY cross-peaks of (Asn4, Thr5), (Thr5, Thr6), and (Ser7, Ala8) as previously shown in Figure 3. Sequence-specific glycosylation-induced conformational change of the polypeptide is the most suitable explanation.

During chemoenzymatic synthesis of the peptide, the carboxyl end of the octapeptide was linked to a solid support via an allylic ester group (Figure 1B). The present structural study indicates that glycosylation at the hydroxyl group of Thr5 induces a conformational change of the polypeptide chain in a sequence-dependent manner. As shown in Figure 10B, molecular dynamics simulations indicate that glycosylation can stabilize a turn-like structure near the glycosylation site. Although no stable well-defined turn can be specified with the current amount of experimentally determined distance constraints, the constraint provided by $d_{\text{NN}}(\text{Thr6, Ser7})$ appears to stabilize the turn structure obtained by simulated annealing experiments. The formation of a turn-like structure would bring the ϵ -NH₂ group

(23) (a) Schutkowski, M.; Bernhardt, A.; Zhou X. Z.; Shen, M.; Reimer, U.; Rahfeld, J.-U.; Lu, K. P.; Fisher, G. *Biochemistry* **1998**, *37*, 5566–5575. (b) Grathwohl, C.; Wuthrich, K. *Biopolymer* **1981**, *20*, 2623–2633.

(24) Rickert, K. W.; Imperali, B. *Chem. Biol.* **1995**, *2*, 751–759.

(25) Hart, G. W. *Annu. Rev. Biochem.* **1997**, *66*, 315–335.

of Lys from the N-terminal region toward the C-terminal end of the peptide, thereby allowing it to function as a general base in the hydrolytic cleavage of the solid support ester bond. Such an effect would resemble the effect of N-glycosylation on the stabilization of the β -turn surface loop from hemagglutinin A, which was detected during a fluorescence energy transfer study.²⁶ Future mechanistic investigation of this model of glycosylation-induced conformational change may further explore this novel activity of glycosylation-induced hydrolytic activity of polypeptides attached to solid supports.

Summary

In this systematic NMR and computer modeling study of an O-SLe^x octapeptide and its synthetic intermediates, we illustrate how a delicate balance between hydrophobic (carbohydrate-polypeptide) and hydrophilic (carbohydrate-carbohydrate and carbohydrate-water) interactions may influence specific glycosylation-induced conformational changes of glycopeptides. Experimental evidence is also presented to indicate the effect of fucosylation on the dynamics of *cis-trans*-proline isomerization. There is no evidence for the presence of an Asx-turn in the studied polypeptide fragment of the mucin domain, even though it contains a potential N-glycosylation site, the Asn-Xaa-Thr motif. This could explain why the mucin domain of MAdCAM-1 presents only O-glycosylated carbohydrates. The glycosylation-induced conformational change of the glycopeptides used in this study provides some insight into the conformational specificity of glycosyltransferases involved in the biosynthesis of O-glycoproteins, and also into glycosylation-induced hydrolytic activity of polypeptides attached to a solid support. Given the problems associated with crystallization of glycoconjugates, NMR methods appear to be preferable to X-ray crystallography for the conformational analysis of complex glycoconjugates.²⁷

Experimental Section

Material and Synthesis. The procedure for the synthesis of the glycopeptide used in this study has been published.⁴ Briefly, the glycopeptide substrate was synthesized on a solid support by using the HYCRON-linker, which enables the removal of acid-labile amino acid side-chain protecting groups while the glycopeptide remains supported. While still attached to the solid support, enzymatic synthesis involving β 1,4-galactosyltransferase, α 2,3-sialyltransferase and α 1,3-fucosyltransferase in the presence of UDP-Gal, CMP-NeuNAc, or GDP-Fuc was then performed to obtain the desired glycopeptides. Pd(O)-catalyzed cleavage of the HYCRON linkage then provided the free glycopeptides. Purification of the products was generally done by GPC (Biogel P4, 0.1M NH₄HCO₃), followed by preparative HPLC (Vydac C18, 250 × 20 mm).

(26) (a) O'Connor, S. E.; Imperiali, B. *Chem. Biol.* **1996**, *3*, 803–812. (b) Imperiali, B.; Rickert, K. W. *Proc. Natl. Acad. Sci. U.S.A.* **1995**, *92*, 97–101.

(27) (a) Wong, S. Y. C.; Guile, G. R.; Dwek, R. A.; Arsequell, G. *Biochem. J.* **1994**, *300*, 843. (b) Homans, S. W. *Prog. Nucl. Magn. Reson. Spectrosc.* **1990**, *22*, 55. (c) Meyer, B. *Top. Curr. Chem.* **1990**, *154*, 141. (d) Berg, J.; Kroon-Batenburg, L. M. J.; Strecker, G.; Montreuil, J.; Vliegthart, J. F. G. *Eur. J. Biochem.* **1989**, *178*, 727. (e) Davis, D. G.; Bax, A. *J. Am. Chem. Soc.* **1986**, *107*, 2820. (f) Kanamori, K.; Roberts, J. D. *Acc. Chem. Res.* **1983**, *16*, 35.

NMR Measurement. One-dimensional and two-dimensional (2D) NMR experiments were performed on a Bruker DRX-600 spectrometer equipped with a 5-mm broadband inverse detection probe at room temperature as reported previously.⁸ NMR spectra were routinely obtained from samples under two different pHs (3.0 and 7.0) in either 99.99% D₂O or 10% D₂O/H₂O. The solution pH was adjusted with appropriate amounts of dilute HCl or NaOH and measured with an Orion 9826 BN electrode before and after each NMR experiment. The reported pH values were direct pH meter readings.

All 2D NMR data were equipped with phase-sensitive mode (TPPI). For 2D TOCSY experiments, the MLEV-17 pulse sequence was used during 65 ms mixing time. A total of 512 *t*₁ data points were collected with 32 transients per *t*₁ and a relaxation delay of 1.5 s. The data were transformed as a 1K × 1K matrix with $\pi/2$ phase shifted sine-bell apodiation applied in both dimensions. For 2D NOESY and ROESY experiments, several mixing times, 100, 200, 300, and 400 ms were used. For samples in 90% H₂O/D₂O, a WATERGATE pulse was used for solvent suppression. We utilized the ROESY experiment to distinguish between NOE cross-peaks and exchange cross-peaks.²⁸

Molecular Modeling and Calculation. Model building and molecular dynamics calculations were performed with an SGI Indigo 2 workstation and Silicon Graphics Power Challenge in the context of the Molecular Simulations Inc. package Insight II and Discover. The AMBER force field (which includes Homans carbohydrate potentials)¹⁵ was used for all calculations. SLe^x was built with the biopolymer module of the Insight package. Molecular modeling calculations were carried out as described below using *J* coupling constants and distance constraints derived from ROESY and NOESY experiments. This structure was further compared to those of published results of conformational studies on SLe^x using MM2 and GESA calculations.⁸ The results were reasonably comparable and enabled us to use the modified AMBER force field, necessary for the modeling of a carbohydrate-peptide hybrid molecule.

The structural model of octapeptide **5** of the mucin domain of MAdCAM-1 was also built with the biopolymer module of the Insight package. Carbohydrate residues were added as appropriate and potentials set to reflect the glycosidic linkage. A total of 11, 52, 43, 44, 51, and 19 experimentally determined interresidue restraints and dihedral angles were applied during the calculations of peptides **1**, **2**, **3**, **4**, **5**, and SLe^x, respectively. The calculation included typical molecular dynamics with initial minimization, randomization of coordinates, 1000 K temperature equilibration, ramping on of restraints, reduction in temperature, and conjugate gradient minimization until a maximum derivative of 0.001 was achieved. Calculations were carried out on structures in vacuo without the explicit inclusion of water molecules. A distance dependent dielectric constant of 4**r* was used. Forty to sixty final structures were obtained for each calculation. In each case no single structure was able to satisfy all experimentally determined NOEs. The conformation of the polypeptide backbone was therefore reported as a set of lowest energy structures whose average conformation satisfies the NOEs.

Acknowledgment. This paper is dedicated to Professor John D. Roberts on the occasion of his 80th birthday, for his profound contributions in physical organic chemistry. This work was supported by grants from NSF (CHE9310081) and NIH (GM44154) to C.H.W. and National Science Council, Taiwan, to W.W.

JA983474V

(28) Davis, D. G.; Bax, A. *J. Magn. Reson.* **1985**, *64*, 533.